

STATUS REPORT AND FUTURE PLANS OF THE INTENSE PULSED NEUTRON SOURCE - ANL

G. H. Lander, J. M. Carpenter, R. L. Kustom, and T. K. Khoe

Argonne National Laboratory  
Argonne, Illinois 60439

Abstract

A brief report is given of the status and current research at the Intense Pulsed Neutron Source (IPNS) at Argonne National Laboratory. Future plans for this facility involve an upgrade of the instruments, the installation of an enriched uranium (booster) target, and the construction of a small accelerator to serve as a prototype for a much more advanced source and, at the same time, deliver five times more protons to the IPNS facility.

Introduction

IPNS has been operating successfully since November 1981, and a number of new areas of science have begun to emerge. Some of these are now documented in the open literature and others are in preparation. Extensive reviews exist in the Proceedings of ICANS-VI<sup>1</sup> (July 1982) and the Yamada Neutron Scattering Conference<sup>2</sup> (September 1982). Other reviews from IPNS<sup>3</sup> are also available to the interested reader. In view of this, we shall confine to a minimum our remarks on condensed matter science now being performed at IPNS and use the remainder of the space to a discussion of future plans. Specifically, these include increasing our instrument capability with the building of an eV spectrometer, a quasielastic spectrometer on the cold source, and a major up-grading of the small-angle scattering diffractometer, also on the cold source. The second stage is the installation of an enriched (booster) target in the IPNS system and the third stage involves the building of a new accelerator, designed to deliver 100  $\mu$ A at 500 MeV.

Present Scientific Activities at IPNS

Much of our emphasis at IPNS is on the use of epithermal neutrons. With the two powder diffractometers<sup>4</sup> a large number of structures are being solved with polycrystalline samples. The unique aspect of these diffractometers is the extremely high resolution ( $\Delta d/d < 0.3\%$ ) which is independent of Q, the momentum transfer, and the availability of a complete Rietveld analysis methodology. An excellent example is given in Fig. 1. Another way of using the high resolution has been on simple systems that have been deformed. Examples here are determinations of residual stress in zircaloy<sup>5</sup> and tungsten carbide cermet<sup>6</sup>. Very small line shifts can be measured corresponding to strains of a few parts in  $10^5$ . The single crystal diffractometer<sup>7</sup> is based on the Laue technique with an Anger type position-sensitive detector<sup>8</sup> and has continued to be used for solving crystal structures<sup>9</sup> and looking at the development of satellite reflections in reciprocal space. An example is given in Fig. 2. The small-angle diffractometer has been used for metallurgy (although until the cold source is operational this is severely limited), biology, and polymer science. An example of a biological program examined is given in Fig. 3. In the field of inelastic scattering the two chopper spectrometers<sup>10</sup> continue to perform extremely well. A major program concerns the study of single particle  $n(p)$  distributions using high energy (500 meV) incident neutrons. So far the most studied system is  $^4\text{He}$  by the group from the University of Illinois.<sup>11</sup> Other interesting experiments concern  $S(Q, \omega)$  distributions in amorphous systems, such as  $\text{SiO}_2$ , illustrated in Fig. 4. Again there are unique features here associated with being able to use very high incident neutron energies, and thus obtain large energy

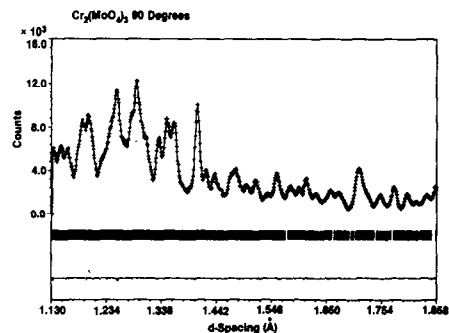


Fig. 1 Neutron diffraction study of chromium molybdate using the General Purpose Powder Diffractometer (GPPD). The + signs are experimental data after background subtraction. The solid curve is the calculated pattern. The vertical ticks show the positions of the independent hkl's in d-spacing. The differences between the data and calculation are plotted in the lower portion of the Figure. (A. K. Cheetham and P. Battle, Oxford University)

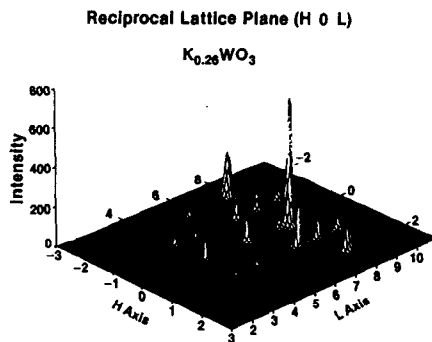


Fig. 2 Reciprocal lattice plane (HOL) of  $\text{K}_{0.26}\text{WO}_3$  as observed below the phase transition with the single-crystal diffractometer. Superlattice reflections can be seen around some of the Bragg peaks and, in addition, there are weak peaks at positions with L odd, which denote a loss of a glide plane in the structural symmetry. Since these were not seen with x-rays they indicate shift of the oxygen atoms (B. Krause and G. Anderson, Northern Illinois University, and A. J. Schultz, ANL)

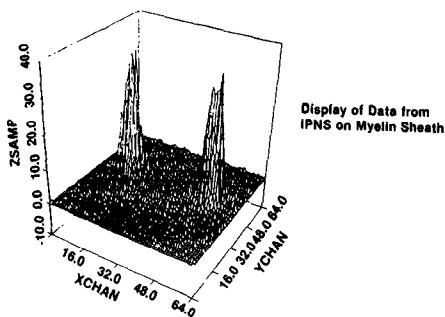


Fig. 3 Display of Data from IPNS on Myelin Sheath  
Bragg peaks from a d-spacing of 87 Å as registered on the small-angle diffractometer from a sample of myelin sheath from a rat sciatic nerve. (D. Worcester and L. Braganza, Institut Laue Langevin, Grenoble)

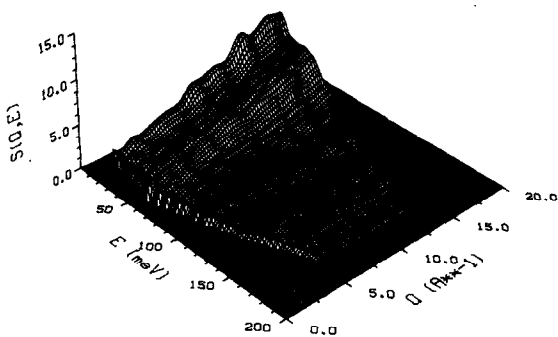


Fig. 4 The dynamic structure factor  $S(Q,E)$  of vitreous  $SiO_2$  at 30 K, measured using the Low-Resolution Medium-Energy Chopper Spectrometer with 218 meV incident neutrons from IPNS. The data exhibit the overall  $Q^2 E^{-2}$  dependence expected for one-phonon scattering; at lowest energy transfers the intensity is due to oxygen atom rocking motions. Peaks at higher energy transfers are due to Si-O-Si group motions. The Q-dependent modulation of intensity contains information about the relative displacements of atoms in each mode of vibration. (J. M. Carpenter, D. L. Price and C. A. Pelizzari)

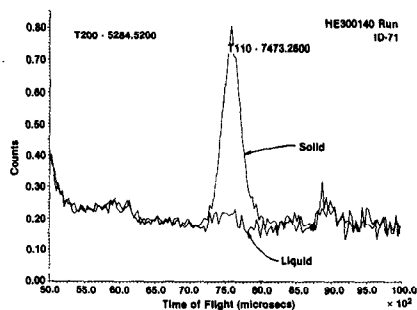


Fig. 5 Spectrum of liquid and single crystal  $^3He$  as recorded in a single detector at the ultra-low temperature facility. The large peak is the (110) Bragg reflection from a crystal of  $^3He$  at 0.010 K. (P. R. Roach, S. K. Sinha, B. K. Sarma and M. Vrtis, ANL and Northwestern University, and K. Skold, Studsvik, Sweden)

transfers,  $\hbar\omega$  or  $E$ , at small momentum transfers  $Q$ . This is particularly important for magnetic problems, since the signal diminishes rapidly with  $Q$ , and a good example is the observation of a crystal-field transition at 130 meV in  $PrO_2$ .<sup>12</sup> The crystal analyzer spectrometer has been primarily used for H-mode spectroscopy. In addition to the above scattering instruments that are open to the user community, there are also 3 special beam experiments at IPNS. The effort on polarized neutrons initially focussed on development of the spin refrigerator, an ingenious method for polarizing a white (polyenergetic) beam of neutrons,<sup>13</sup> and is now being set up to measure the change in refractive index superconductors as a function of neutron wavelength and thus field penetration.<sup>14</sup> A large collaborating group is attempting to measure the nuclear spin ordering in  $^3He$  below 1 mk. They recently succeeded in growing single crystals of  $^3He$  and seeing a Bragg reflection, convincingly demonstrated in Fig. 5. Another effort is aimed at producing ultra-cold neutrons from a pulsed source by Doppler-shifting the neutrons with a large d-space mica crystal.<sup>15</sup>

The substantial effort on radiation damage at IPNS will not be discussed here, as it is covered in detail by Kirk in these Proceedings.

#### Future Plans in Scattering Instruments

The most immediate need at IPNS for the SAD, polarized beam and  $^3He$  projects is a cold source. Our first attempt at a cooled (20K) methane moderator was not successful. We will have an 80K moderator source operating in October 1983 and are planning a new low-temperature moderator. The 80K moderator will already provide a substantial gain in the longer (4-6 Å) wavelength neutrons. [See paper by A. W. Schulke et al. in this Proceedings.]

At present, construction is taking place on the eV spectrometer designed to use high energy neutrons ( $> 1$  eV) by counting secondary particles (initially  $\gamma$ -rays from the 4.28 eV Ta resonance) when the n- $\gamma$  reaction takes place in a thin absorbing foil. Optimum use has been made of experience with machines of this kind at Harwell<sup>16</sup> and KENS, Japan,<sup>17</sup> although it should be realized that this kind of neutron spectroscopy is completely new. The ANL spectrometer should be operational late in 1983.

A new instrument to be built at IPNS is a quasielastic spectrometer. Plans for this are now in a preliminary state. This technique has been of special significance in chemical studies, often complementing either NMR or conventional neutron spectroscopy. At KENS the quasielastic machine, LAM-II, is based on inverse geometry with graphite monochromators and has a resolution of  $\sim 20 \mu eV$ .<sup>18</sup>

#### Target Development

With present proton currents (12  $\mu A$ ) and currents we envision in the near future ( $\sim 16 \mu A$ ), the heat-transport capabilities of the depleted-uranium targets and cooling systems of IPNS are not severely taxed. (They were designed<sup>19</sup> to operate with maximum center temperatures of 330°C at a current of 22  $\mu A$  of 500 MeV protons.) We have begun an effort to provide higher neutron production rates and higher neutron fluxes by installation of a  $^{235}U$ -enriched target.

Preliminary studies based on HETC-VIM calculations, indicate that a target identical in size to the present ones, decoupled from surroundings to maintain a short response time by  $1.7 \times 10^{22} \text{ }^{10}B/cm^2$  and with 65%  $^{235}U$ , would have an effective multiplication

factor  $k_{eff} = 0.82$ , thus a nominal prompt-neutron gain factor  $G = 1/(1-k_{eff}) \sim 5$ . The pulse shape determined from the Monte Carlo simulations is not significantly broadened for energies below about 100 eV. The increase, above that for the depleted-U case, in slow-neutron beam current is about a factor 3.5. This is presumably because the distribution of primary spallation source neutrons is not identical to that of the fundamental multiplying mode of the booster. We estimate that the total power in the target would be about 100 kW for such a booster. Addition of about 1%  $^{149}\text{Sm}$  to the alloy eliminates conclusively the possibility of thermal criticality. More-detailed KINO code studies now in progress indicate that  $k_{eff} \sim 0.95$  if the  $^{10}\text{B}$  layer were not present - we expect this to be a significant safety question. We find that the main influence upon the generation time is the water surrounding the target, with the specified  $^{10}\text{B}$  layer, the prompt neutron generating time is 30 nsec. Assuming a total 100 kW power, distributed in part as in the depleted-U target and the remainder as in the fundamental booster mode, requires a minimum disk thickness of 12 mm. This minor reduction from 25 mm is due to the broader power-density distribution in the booster case. Fabrication procedures identical with those used for depleted uranium disks should be appropriate. Detailed studies of a loss-of-coolant occurrence indicate that the multiplying target cannot reach a temperature such as to melt the uranium (1100 C) or zircaloy cladding. Indications are that sufficient margin may exist in this respect, so that loss of coolant need not preclude continued use of the target. Delayed neutrons will increase from their present fraction (assumed to be the same as in ZING-P) of 0.0053 to about 0.03, and we expect this to be tolerable background in most experiments since no instrument scientists have yet sensed any effect of the present delayed-neutron level. The additional neutrons will require only minor shielding changes (mostly at choppers and beam stops) since the neutron gain is entirely in easily-stopped fission neutrons.

Technical studies now in progress are aimed to refine the calculation of the loss-of-coolant temperature transient, to optimize the coupling of booster to the primary source (by changing target dimensions) and estimate more accurately the power density distribution and slow-neutron beam currents. Safety-and-security-related studies planned to begin shortly will address questions of criticality and security during fabrication, assembly and installation.

Detailed design will follow completion of these preliminary analysis and has not begun. A somewhat-optimistic estimate of the time when the booster will be installed is in early calendar year 1985.

#### Argonne Super Pulsed Spallation Neutron Source

Argonne Super Pulsed Spallation Neutron Source (ASPUN)<sup>20</sup> is a facility concept being studied at Argonne that would provide greater than  $10^{17}\text{n/cm}^2\text{-sec}$  in the 1 eV range. ASPUN is described in another paper at this conference. Argonne has concluded that a small-scale prototype could be built onto the IPNS facility affording critical tests of the principal ASPUN ideas and at the same time make an important increase in the scientific capabilities of IPNS.

The Mini-ASPUN plan uses a 500 MeV Fixed-Field Alternating Gradient (FFAG) accelerator<sup>21</sup> as the proton source. An FFAG accelerator has dc excited magnetic fields which increase with radius as  $(R/R_0)^k$ . Beam is injected into the inner radius, and as it is accelerated the equilibrium orbit radius grows to a larger value. Frequency modulated rf cavities are

used to accelerate the beam following a voltage and frequency program that tracks the beam energy. The final energy is reached at the maximum radius, and beam is extracted in one turn.

Mini-ASPUN uses the IPNS 50 MeV Linac, 50 MeV transport line, 500 MeV transport line, and target. A plan view of the IPNS facility with the 500 MeV FFAG drawn in place is shown in Fig. 6. The design goal for the average proton current of the 500 MeV FFAG is 100  $\mu\text{A}$ .

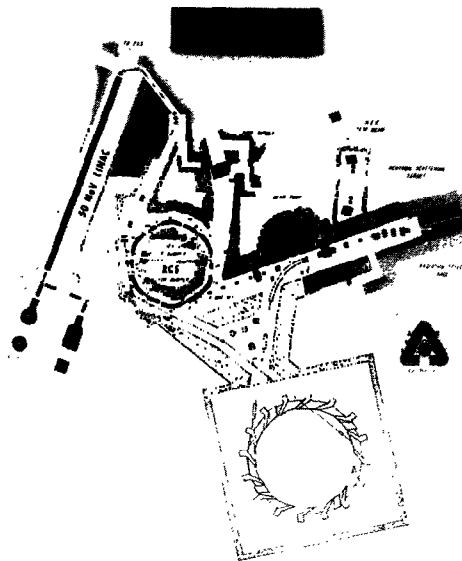


Fig. 6 Schematic of the proposed IPNS System including the mini-FFAG.

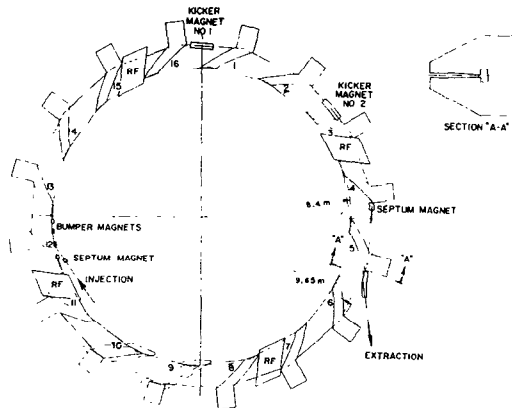


Fig. 7 Schematic of the 500 MeV FFAG ring.

A plan view of the 500 MeV FFAG ring is shown in Fig. 7. A table of parameters is given in Table 1. A total of 16 magnets are equally spaced around the ring. The combination of the entrance and exit edges and the field gradient in the magnet generates the transverse focusing in the vertical and horizontal planes. Each magnet and straight section corresponds to one cell of an accelerator lattice that is a DFFO configuration in the horizontal plane. Since there are sixteen magnets, there are sixteen identical lattice cells.

The injection scheme is  $H^- \rightarrow H^+$  stripping using four bumper magnets and a septum magnet. A plan view of the injection is shown in Fig. 8. The dashed line indicates the normal unperturbed equilibrium orbit. The dot-dash line indicates the perturbed or bumped orbit produced by the four bumper magnets. The bumper magnet and septum magnet fields are reduced during injection to spread the beam more uniformly in space to reduce the space charge effect.

Table 1. FFAG for Mini-ASPUN

Injection Energy	50 MeV
Extraction Energy	500 MeV
Injection Radius	8.4 m
Extraction Radius	9.65 m
Injection Field	0.489 T
Extraction Field	1.5 T
Number of Sectors	16
Angular Width of Sectors	5.625°
Field Index, $k$	8
Spiral Angle, $\xi$	57°
Radial Betatron Frequency, $\nu_r$	3.25
Vertical Betatron Frequency, $\nu_z$	2.3
Space Charge Limit	$4 \times 10^{12}$
Radial Beam Emittance @ 50 MeV	$170 \pi \text{ mm-mr}$
Vertical Beam Emittance @ 50 MeV	$120 \pi \text{ mm-mr}$
Frequency Range	1.784-3.748 MHz
Maximum RF Voltage per Turn	60 kV
Harmonic Number	1
Average Current	100 $\mu\text{A}$
Repetition Rate	180 Hz

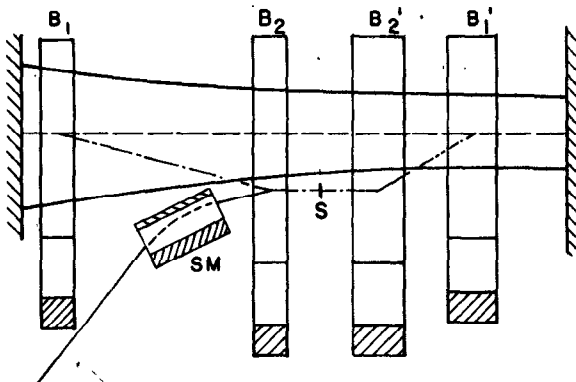


Fig. 8 Injection system showing four bumper magnets (B), Septum Magnet (SM), and Stripper Foil (S).

The 50 MeV linac would be operated at 180 Hz with a short beam pulse of about 50  $\mu\text{sec}$ . The space charge limit is  $4 \times 10^{12}$ . The rf voltage and frequency programming technique will be the same as that described for the 1100 MeV FFAG in the full sized ASPUN except that only 60 kV total rf voltage is needed. This will be accomplished with four rf cavities spaces around the ring as shown in Fig. 7. The injection radius is 8.4 m and the extraction radius is 9.65 m. The spiral angle is 57° and the angular width of each magnet is 5.625°. The magnetic field in the magnet increases with average radius by the amount  $B = B_0 (R/R_0)^8$ . The repetition rate will be 180 Hz. Internal stacking will be done by merging six pulses so that the extraction repetition rate will be 30 Hz. The betatron tune in the horizontal plane is 3.25 and in the vertical plane is 2.3. The magnetic field at the injection radius is 0.489 T and at extraction radius is 1.5 T. The magnet gap is 18 cm out to the 9.0 m radius, then contracts to 9 cm at the outside edge of the magnet.

One turn extraction will be accomplished using fast ferrite kicker magnets on the outside edge of the ring. The kicker magnet shown in straight section 16 of Fig. 7 kicks the beam inwards by 10 mrad. The beam undergoes an inward betatron oscillation for half a period. The second kicker magnet in straight section 2 produces an outward kick of 10 mrad. The extracted beam then enters the septum magnet in straight section 4 and finally the bending magnet outside of straight section 5. The pulse width will be about 140 nanoseconds. The fast ferrite kicker magnets are each 1 meter long and operate with 0.019 T-m integrated B-dl field. The septum magnet is 0.7 m long and operates with a 0.23 T field.

Several important elements of the full-sized ASPUN project will be tested on Mini-ASPUN. In particular, these include the development of magnets, highly efficient adiabatic capture, acceleration, and extraction, and internal stacking.

Transverse focusing of the beam in the ASPUN accelerator is provided by a combination of the entrance and exit edge angles and a radial gradient of the magnets. It is essential in the design of the machine that the fringing fields and edges can be accurately controlled so that the transverse betatron oscillations are sufficiently constant to avoid beam loss due to resonances. There are good reasons to believe that necessary accuracy can be achieved by coil shaping, shimming, and edge coils. Mini-ASPUN will provide the opportunity to test these various techniques and to determine the most flexible and easily controllable combination.

The injection efficiency needs to be exceedingly good or effective beam loss collectors need to be developed to avoid irradiation and damage to the machine components. Mini-ASPUN will provide the opportunity to perfect the rf voltage and frequency hardware and control to achieve theoretical predictions or to develop alternative approaches.

Beam stacking is required to reduce the external beam repetition rate of the ASPUN accelerator to a rate ( $\sim 30 - 100 \text{ Hz}$ ) that is desired by many of the solid state science experimenters. Again, Mini-ASPUN provides an excellent research vehicle to develop this technique.

Mini-ASPUN will allow the development, testing, and demonstration of almost all elements of the full ASPUN facility. Benefits to the full ASPUN facility will accrue in not only the technical and economic elements but also in the speed at which the full design goals can be achieved after completion of construction. To the neutron scientists, this would represent a factor of five increase in intensity over the upgraded IPNS facility.

#### References

1. Proceedings of the ICANS-VI meeting at Argonne National Laboratory, July 1982, ANL Report ANL-82-80 (1982).
2. G. H. Lander, *Physica* 120B 15 (1983).
3. The IPNS User Bulletin is published twice a year; a Progress Report for 1981 - 1983 is in preparation. To obtain these documents and be placed on our mailing list write to the Scientific Secretary, IPNS-360, Argonne National Laboratory, Argonne, Illinois, 60439.
4. J. D. Jorgensen and J. Faber, in Ref. 1, p-105, (1982).
5. S. R. MacEwen, J. Faber, and A. P. L. Turner, *Acta Metall* 31, 657 (1963).
6. A. Kravitz, unpublished.

7. A. J. Schultz, R. G. Teller, and J. M. Williams, in Ref. 1, p. 115 (1982).
8. A. J. Schultz, R. G. Teller, J. M. Williams, M. G. Strauss, and R. Brenner, *ACA Transactions* 18 169 (1982).
9. A. J. Schultz, R. G. Teller, M. A. Beno, J. M. Williams, M. Brookhart, W. Lamana, and M. B. Humphrey, *Science* 220, 197 (1983).
10. D. L. Price, J. M. Carpenter, C. A. Pelizzari, S. K. Sinha, I. Bresof, and G. E. Ostrowski, in Ref. 1, p. 207 (1982).
11. R. O. Hilleke, P. Chaddah, R. O. Simmons, D. L. Price, and S. K. Sinha (to be published).
12. S. Kern, C.-K. Loong, J. Faber and G. H. Lander, *Solid State Comm.* (in press).
13. G. P. Felcher in Ref. 1, p. 179 (1982).
14. S. D. Bader, G. P. Felcher, K. E. Gray and R. T. Kampwirth, *Physica* 120B, 219 (1983).
15. J. W. Lynn, W. A. Miller, T. W. Dombeck, G. R. Ringo, V. E. Krohn and M. S. Freedman, *Physica* 120B, 114 (1983).
16. "Pulsed Neutron Scattering" by C. G. Windsor, Taylor & Francis, London, 1981.
17. J. M. Carpenter, N. Watanabe, S. Ikeda, Y. Masuda, and S. Sato, *Physica* 120B, 126 (1983).
18. N. Watanabe, H. Sasaki, Y. Ishikawa, Y. Endoh, and K. Inoue, in Ref. 1, p. 16 (1982).
19. J. M. Carpenter, U. Ahmed, J. R. Ball, F de Sousa, and T. Ewing, Argonne National Laboratory Report ANL-83-11 (1983).
20. T. K. Khoe and R. L. Kustom, *IEEE Transactions on Nuclear Sciences*, NS-30, (August, 1983).
21. F. T. Cole, R. O. Haxby, L. W. Jones, C. H. Pruett, and K. M. Terwilliger, *Review of Sci. Inst.* 28, 403 (1957).